INFLUENCE OF SHIELDING GASES ON STUD WELDING

Álisson Fernandes da Rosa[1]
Leonardo Matos Brasil[2]
Filipe Freitas Targino[3]
Alberto Bonamigo Viviani[4]
Régis Henrique Gonçalves e Silva[5]
Federal University of Santa Catarina
[1]alisson.fernandes@posgrad.ufsc.br
[2]matos.brasil@grad.ufsc.br
[3]filipe.targino@grad.ufsc.br
[4]alberto.bonamigo@labsolda.ufsc.br
[5]regis.silva@ufsc.br

Abstract. *Stud welding is an electric arc welding process used to quickly and efficiently attach studs and other metallic components to sheets or structural parts. It is widely applied across industrial sectors such as civil construction, shipbuilding, automotive, and petrochemical industries. The process involves generating an electric arc between the stud and the base material to melt the contact surfaces and join them under pressure. A critical factor influencing weld quality is the choice of shielding gas, which affects arc behavior and the characteristics of the resulting weld. This study investigates the impact of different shielding gases — pure CO_2, pure helium, pure argon, and the C15 mixture (85% argon and 15% CO_2) — on the stud welding process. The analysis focuses on the physicochemical properties of each gas and their effects on arc stability, energy input, and weld morphology. The results offer valuable insights for selecting the most suitable shielding gas for different applications and welding requirements, contributing to process optimization.*

Keywords: *stud welding, shielding gases, gas properties*

1. INTRODUCTION

Stud welding is a process of joining metallic fasteners using an electric arc. The arc is generated by a gun that performs a retracting and advancing motion toward the workpiece. This movement creates an electric arc that produces localized fusion between the tip of the stud and the surface of the base metal. After a predefined time interval, the stud advances against the workpiece, establishing the required metallurgical bond. The stud welding technique is characterized by the use of high electric currents and mechanical pressure applied over a short period, promoting the bonding between the stud and the base metal. Some process variants eliminate the need for shielding gas by using a ceramic ferrule around the welding area. During fusion, the ferrule confines atmospheric air and expels excess gases through vents, ensuring greater process stability. In conventional variants, shielding gas is employed—typically mixtures of argon and carbon

dioxide—especially for welding carbon steels. Stud welding (SW) is widely used in sectors such as automotive, civil construction, and the oil and gas industry (Trillmich & Welz, 2016).

Shielding gas is a critical component in the stud welding process, playing a vital role in ensuring weld quality and integrity. Its primary function is to protect the weld pool (the molten metal during welding) and the electric arc from atmospheric contamination. Without adequate protection, oxygen and nitrogen in the air can react with the molten metal, resulting in undesirable defects such as porosity (small holes or voids in the weld) and oxidation-induced embrittlement, which compromise the strength and durability of the welded joint (Trillmich & Welz, 2016). In addition to preventing atmospheric contamination, shielding gas significantly influences the stability and characteristics of the electric arc, directly affecting weld quality. It ionizes the path between the stud and the workpiece, facilitating the conduction of electric current and generating the heat necessary for fusion. The gas composition impacts the ion density within the arc, which, in turn, affects voltage and energy distribution—thereby influencing penetration, weld bead shape, and spatter levels.

This study aims to investigate the impact of different shielding gases—pure CO_2, pure helium, pure argon, and the C15 mixture (85% argon and 15% CO_2)—on the stud welding process. The research focuses on a detailed analysis of how each gas's properties affect arc stability and weld morphology. A comprehensive evaluation of the results seeks to provide valuable insights into selecting the optimal shielding gas for various applications and welding requirements, contributing to overall process optimization.

2. MATERIALS AND METHODS

In this study, a BMK-16i direct current (DC) inverter power source from SOYER was used. This equipment is capable of welding studs with diameters ranging from ⌀6 to ⌀20 mm, delivering up to 1000 A of current for a maximum duration of 1000 milliseconds. It was paired with a PH-3N weld gun, featuring a solenoid-driven movement mechanism that allows precise adjustments for stud retraction and protrusion. The materials used included ⌀10 mm carbon steel studs from SOYER, grade 4.8, with a chemical composition of up to 0.55% carbon, 0.05% phosphorus, and 0.06% sulfur. Additionally, SAE/AISI 1020 steel plates were employed, with dimensions of 6.35 mm in thickness, 76.2 mm in width, and 4 meters in length. Data acquisition was carried out using the 3SR device developed by IMC Welding, which measured current, voltage, displacement, and temperature at a frequency of 5,000 Hz. Hall effect sensors were used for current measurement, linear displacement sensors for displacement, and type K thermocouples for temperature.

Welding was performed in series of ten for each shielding gas: pure argon, pure CO_2, pure helium, and the C15 gas mixture (85% argon and 15% CO_2), while keeping all welding parameters constant (Welding current: 800 A, Lift: 1.5 and Protrusion: 2.0 mm). The average instantaneous energy was calculated from the current and voltage data acquired during the process. The backside temperature of the plates was measured using a thermocouple aligned with the fastening stud. Weld evaluation included metallographic analysis to determine penetration depth and weld spread area. To complement the study, high-speed filming was performed using an IDT Motion Pro Y4S2 camera, paired with a CAVITAR/Cavilux HF laser illumination system.

3. RESULTS AND DISCUSSIONS

3.1. Pilot Arc for Different Gases

The pilot arc period is essential for initiating the electric arc in the stud welding process. Upon pulling the trigger, the stud remains in contact with the plate for 0.1 seconds, allowing a short-circuit current of 80 A to flow. After this interval, the stud begins to retract from the plate, establishing the pilot arc with the same current intensity (80 A). In Figure 1, the average values obtained were compiled into a single graph to enable direct comparison among the four shielding gases studied. The variations observed may be associated with the physicochemical properties of each gas, which influence the ionization process.

The results reveal similar ignition and pilot arc behavior for pure CO_2 and pure argon, which can be attributed to their comparable ionization potentials, resulting in analogous arc initiation characteristics. In contrast, the increased voltage observed for C15 is explained by its instability—a behavior typical of CO_2-containing mixtures. According to Zielinska et al. (2008), variations in arc voltage when using pure argon and gas mixtures with small CO_2 additions (less than 3%) are related to enhanced plasma conductivity.

Pure helium, due to its high ionization potential and thermal conductivity, requires significantly more energy to initiate arc formation. This leads to higher voltage peaks during ignition. Regarding the electric current behavior, a decay effect was observed in all cases when the stud reached its maximum retraction. This phenomenon is associated with increased electrical resistance in the atmosphere at the moment the arc opens. As the stud moves away from the workpiece, the distance between the electrode and the base material increases, raising the resistance of the gaseous medium. Consequently, the welding power source detects the higher resistance, leading to a reduction in current flow—thereby causing current decay.

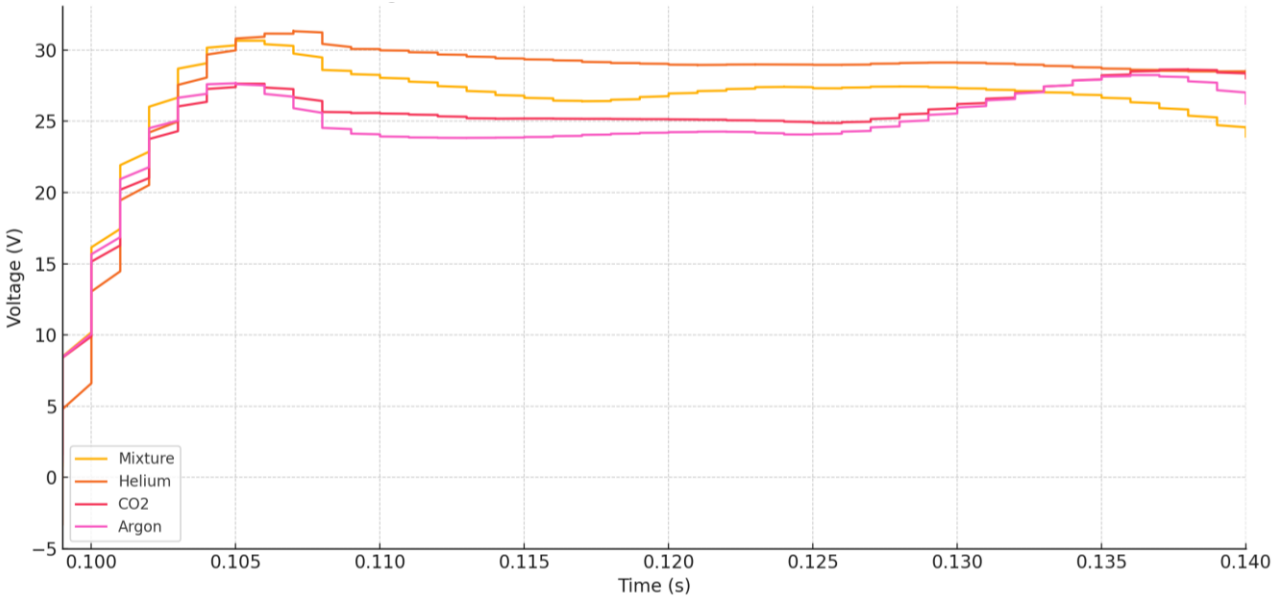

Figure 1 *- Average Pilot Arc Voltage for Different Gases*

3.2. Main Arc for Different Gases

Following the same approach used for the pilot arc analysis, the main arc behavior was evaluated. The average voltage values for each shielding gas were consolidated into a single graph (Figure 2). As shown, pure CO_2 and pure

helium exhibited higher voltage requirements to sustain arc ionization. In the case of CO_2, this behavior is associated with endothermic dissociation and ionization reactions, which demand significant energy input. For pure helium, its high ionization potential and elevated thermal conductivity account for the increased energy needed to maintain a stable arc.

In contrast, pure argon has a low ionization potential, which facilitates both the formation and maintenance of a stable arc, requiring less energy to ionize the atoms. Furthermore, its low thermal conductivity minimizes heat dissipation to the surrounding environment, thereby concentrating thermal energy within the arc region.

Regarding the C15 mixture, instability patterns similar to those observed in the pilot arc were identified. However, when these instabilities were averaged, the mean voltage was close to that of pure argon. This phenomenon is attributed to the combined effects of CO_2—responsible for surface oxidation and electron field emission—and argon, whose low ionization potential supports efficient ionization. As a result, the interaction between these gases in the C15 mixture yields an average voltage similar to that of argon, despite its fluctuating arc behavior.

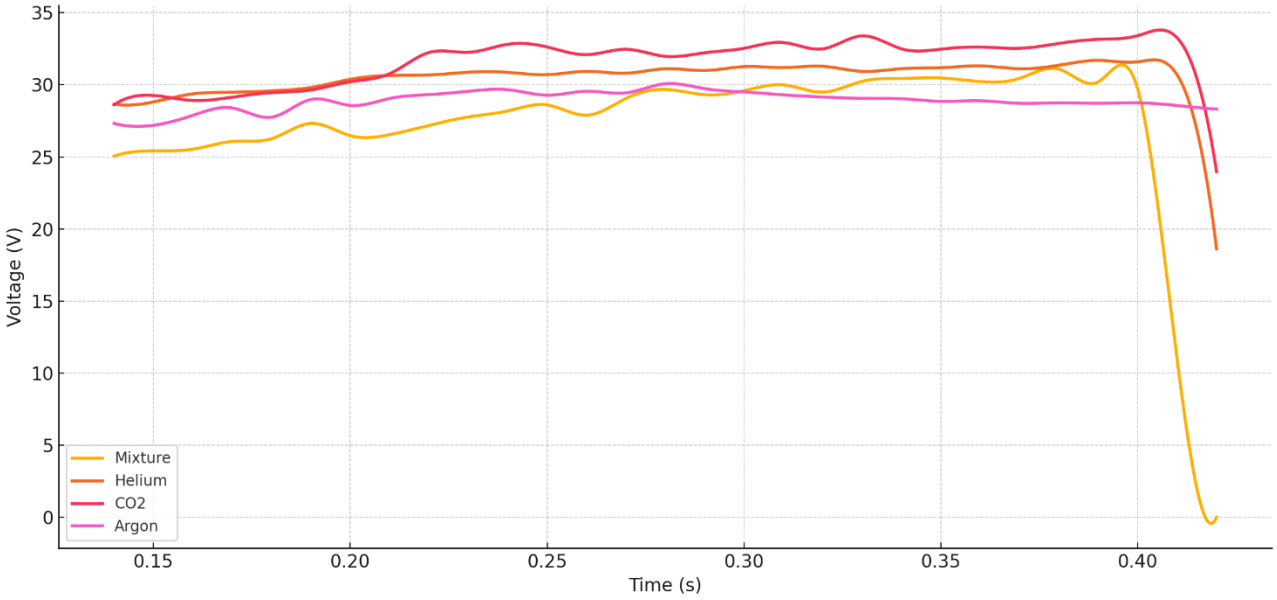

Figure 2 *- Averages of the main arc voltage for different gases*

3.3. Voltage Heatmap for Different Gases

Figure 3 presents the ten voltage acquisitions recorded throughout the entire welding period for each shielding gas, compiled into a single heatmap per gas. Each acquisition is arranged horizontally over the pilot arc interval (0.10–0.14 seconds), resulting in the stacking of ten measurements within a single graph. The color gradient represents voltage intensity, ranging from the minimum to the maximum values, thereby facilitating the visualization of arc stability and repeatability. The heatmap analysis clearly illustrates the voltage stability and repeatability associated with each gas. Pure argon shows consistent performance, maintaining a stable voltage around 27.5 V, with only minimal indications of short circuits. CO_2, in contrast, displays initial instability in the main arc, with fluctuations between voltages of approximately 27.5 V and peaks reaching 35 V, suggesting frequent short circuit events. For pure helium, voltage remains stable around 32.5 V, with no short circuits observed throughout the measurements. On the other hand, the C15 mixture exhibits pronounced instability, characterized by a predominance of short circuits during the welding cycle, as indicated by abrupt voltage variations.

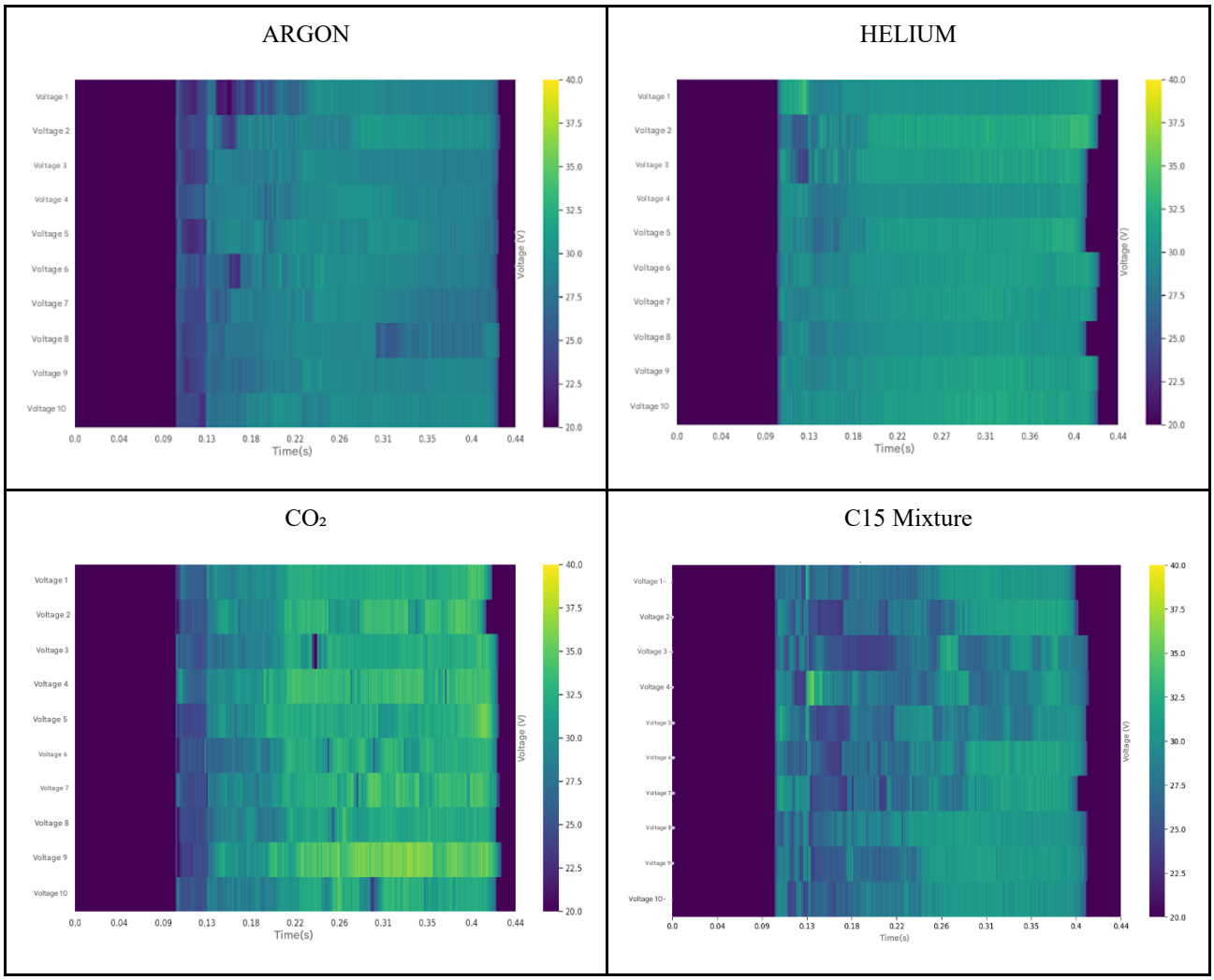

Figure 3 *- Voltage Heatmap for Different Gases*

3.4. Welding Energy for Different Gases

The calculation of average instantaneous energy was performed as described in the Materials and Methods section. The combined energy values for the pilot arc and main arc are presented in Figure 4, corresponding to each acquisition conducted using the different shielding gases. Analysis of the results shows that the average instantaneous energy varies between acquisitions even when using the same gas. This behavior is consistent with the voltage fluctuations observed in the heatmaps, which reflect variations in arc stability. Such energy variability may be attributed to the movement of molten material at the tip of the stud, which directly influences the electric arc dynamics.

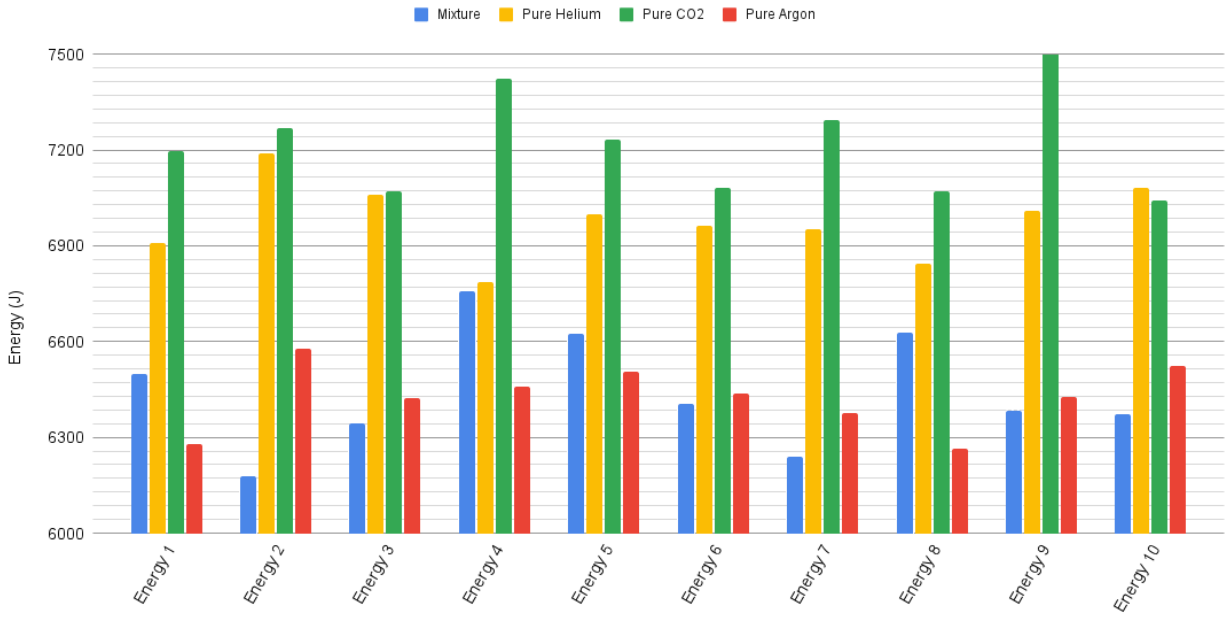

Figure 4 *- Average instantaneous energy for each acquisition*

The average energy values for both the pilot arc and main arc were calculated and are presented in Tables 1. It was initially observed that the pilot arc exhibits very low energy values, representing less than 1% of the total energy supplied to the process. The purpose of the pilot arc is generally not fusion. In specific situations, for instance, to remove surface impurities, it may be advisable to allow the pilot arc to act on the workpiece surface with a higher current Trillmich and Welz (2016). This finding reinforces the understanding that the pilot arc functions primarily as an auxiliary arc.

The analysis of the energy supplied during the main arc reveals that carbon dioxide (CO_2) and helium result in significantly higher energy levels compared to the C15 mixture and pure argon. For example, when using pure CO_2, the average energy delivered during the main arc increases by approximately 800 J compared to pure argon and the C15 mixture. Similarly, helium results in an increase of around 500 J relative to the same gases. This phenomenon is attributed to the voltage behavior during the main arc, where both CO_2 and helium maintain higher voltage levels throughout the welding process. Since the electric current remains constant for all gases, higher voltages naturally lead to greater energy input into the weld.

Table 1. *Average instantaneous energy, standard deviation, and percentage standard deviation during the main and pilot arc for different gases*

Gas	Pilot Arc Energy (J)	Pilot Arc Std Dev	Pilot Arc % Std Dev	Main Arc Energy (J)	Main Arc Std Dev	Main Arc % Std Dev
CO_2	28,79	0,77	2,674	7240,84	200,7	2,7717
Helium	29,89	1,02	3,4125	6987,59	117,8	1,6858
Argon	27,2	0,53	1,4985	6434,03	100,12	1,5561
C15	27,74	0,43	1,5591	6443,17	182,5	2,8324

3.4.1 Average Instantaneous Energy - Pilot Arc

During the pilot arc phase, the current flow remains low, while the voltage is relatively high, resulting in a low-intensity arc, as recorded in Figure 5. However, distinct arc behaviors were observed depending on the shielding gas used. For helium and argon, cathodic cleaning was initiated, generating a rotational arc that seeks cathodic spots, with no fusion occurring at the stud tip. In contrast, when using carbon dioxide (CO_2), the arc immediately anchored itself at the beginning of the retraction movement, leading to slight fusion at the stud tip. For the C15 gas mixture, a hybrid behavior was observed, combining initial cathodic cleaning with an anchored arc, which intermittently attempts to shift between cathodic spots.

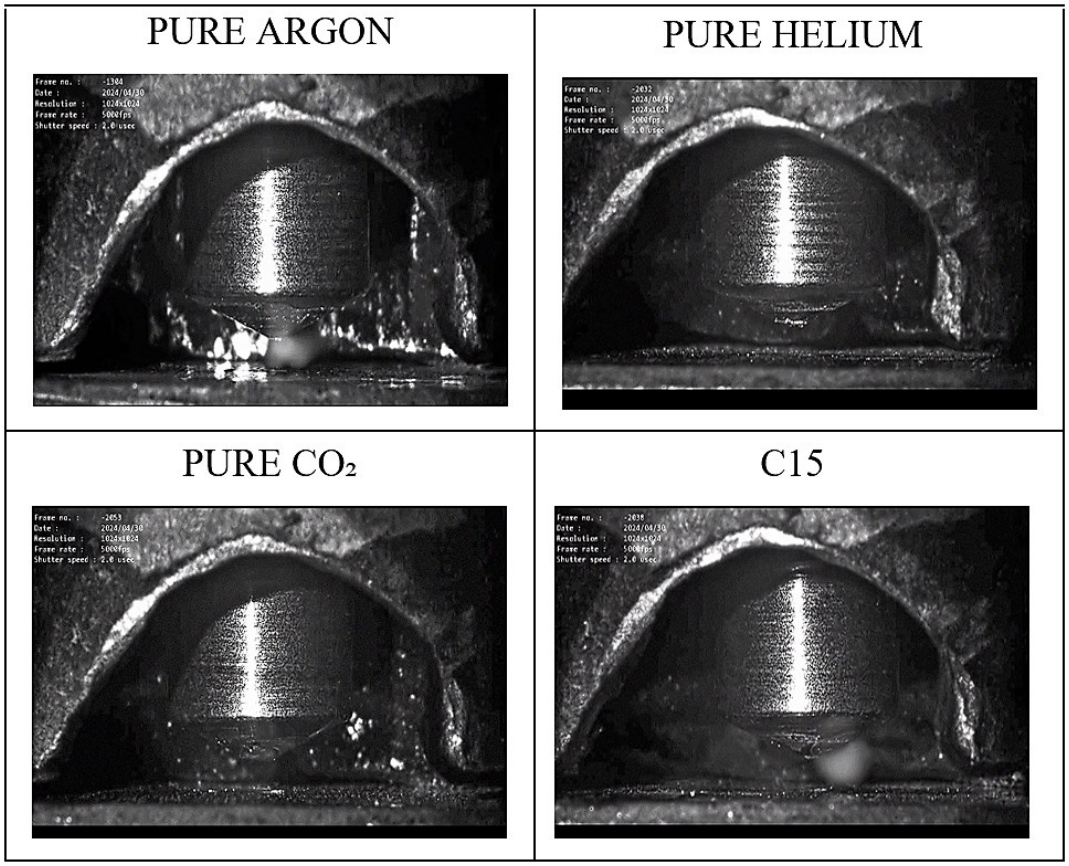

Figure 5 *- High-speed filming during the pilot arc*

3.4.2 Average Instantaneous Energy - Main Arc

The high-speed footage captured for pure argon is presented in Figure 6. A high degree of cathodic cleaning and low fluidity of the molten tip were observed, effectively preventing short circuits. In regions where cathodic cleaning occurred, arc scaling was detected, leading to localized surface fusion. This behavior suggests that the supplied energy was not concentrated at a single point but rather distributed across the surface, expanding the fusion area. Such a mechanism helps prevent the formation of regions with excessive heat accumulation, contributing to more uniform thermal distribution.

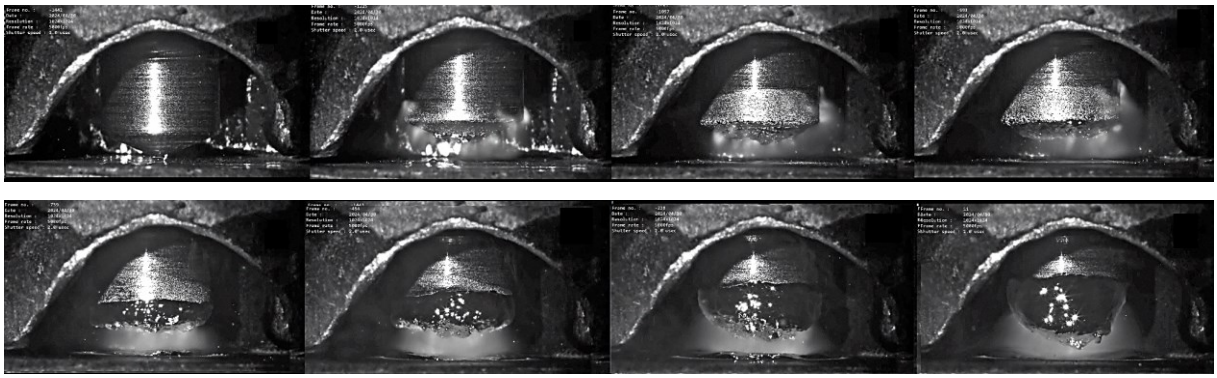

Figure 6 *- High-speed filming for pure argon*

The high-speed footage captured for pure helium is shown in Figure 7. The images reveal that helium initiates cathodic cleaning, but with lower efficiency compared to argon (Figure 6). This difference is attributed to the higher ionization potential of helium, which makes argon more effective in sustaining cathodic cleaning. As a result, in helium-based welding, it is more efficient to maintain an already established arc, reducing the need for repeated arc initiation. Due to the limited cathodic cleaning effect, the electric arc concentrates more energy at the stud tip, leading to greater material fusion. Additionally, the increased arc intensity lowers the surface tension of the molten metal, enhancing fluidity compared to argon.

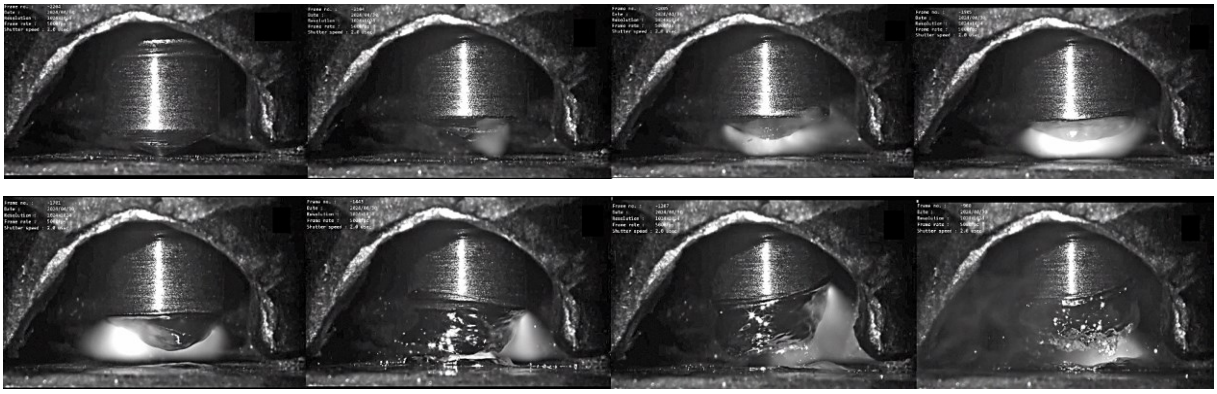

Figure 7 *- High-speed filming for pure helium*

Figure 8 presents the high-speed footage recorded using pure CO_2. Unlike argon, carbon dioxide (CO_2) did not induce cathodic cleaning during the pilot arc phase. Instead, the arc remained anchored throughout this stage, ensuring stability until the transition to the main current. This behavior resulted in pronounced fusion at the anchoring point, promoting a high degree of material melting and a rapid temperature increase from the beginning of the process. Additionally, CO_2 contributed to greater fluidity at the molten tip by reducing the surface tension of the liquid metal. Due to this high material fusion, vaporization forces increased significantly, causing the molten metal at the electrode tip to be pushed upward.

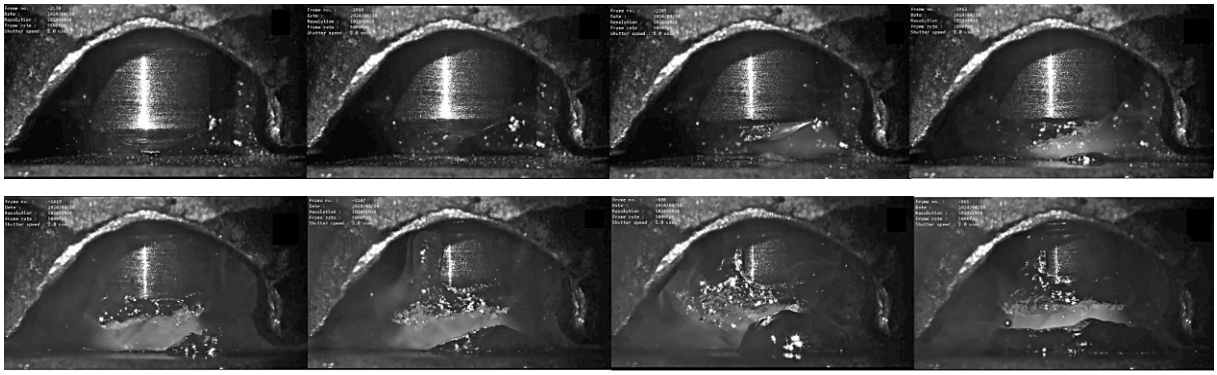

Figure 8 *- High-speed filming for pure CO_2*

The high-speed footage captured for the C15 gas mixture is shown in Figure 9. During welding with C15, an intensification of the arc was observed after a certain period. Initially, the molten droplet exhibited behavior similar to that of pure argon, displaying low fluidity and a stable electric arc. However, over time, the arc intensified, leading to greater disturbance of the molten droplet. As seen in Figure 9, arc stepping due to cathodic cleaning did not occur. Throughout the entire process, the arc remained anchored at the stud tip, promoting a higher degree of fusion and generating a larger volume of molten material. The addition of 15% CO_2 lowered the surface tension, increasing the fluidity of the molten material at the stud tip. The instability of the C15 mixture can be attributed to arc movement between cathodic points induced by CO_2. This increased fluidity favored the occurrence of short circuits, which momentarily interrupted the arc, forcing its reignition.

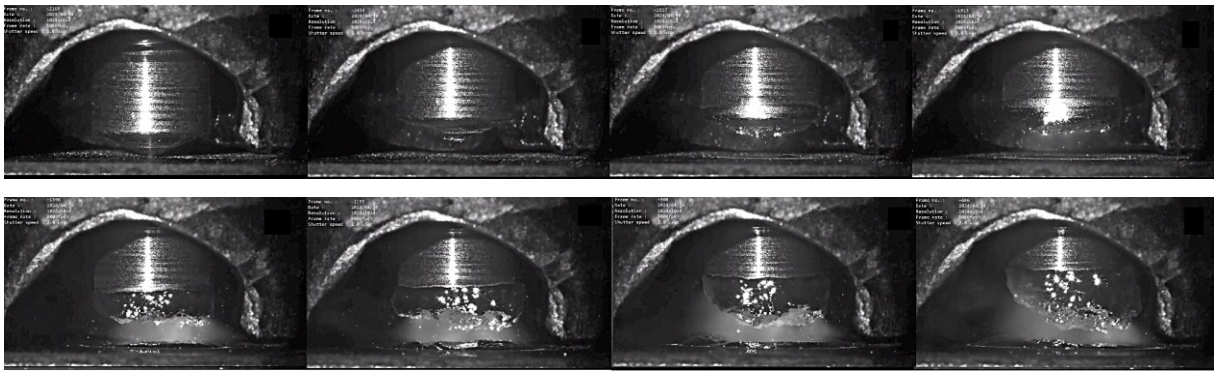

Figure 9 *- High-speed filming for C15*

3.5. Penetration Depth for Different Gases

Based on the results of the macrographs, the penetration values were organized in Table 2. Pure CO_2 demonstrated the highest average penetration, followed by helium, the C15 mixture, and finally pure argon. Pure CO_2 stood out by showing the greatest penetration due to its higher welding energy, while helium and the gas mixture also exceeded pure argon. Although pure argon and the mixture had similar energy levels, the mixture presented, on average, 0.14 mm more penetration, reinforcing the positive effect of CO_2 in the mixture, which enhances fusion, as shown in the high-speed footage.

Table 2. *Penetration calculation results for different gases.*

Gas	Sample 1 (mm)	Sample 2 (mm)	Sample 3 (mm)	Average (mm)
CO_2	2.518	2.184	2.444	2.382
He	1.822	1.742	1.939	1.834
C15	1.773	1.742	1.654	1.723
Ar	1.617	1.596	1.538	1.583

3.6. Welding Collar Formation

The formation of the weld collar occurs through the simultaneous fusion of the stud and the sheet, both in a liquid state. This union takes place when the stud plunges into the molten pool, merging the two components. As illustrated in the high-speed footage, pure CO_2 exhibits higher wettability, allowing the molten material from both the stud and the sheet to spread more effectively, resulting in a shallower and more widely distributed weld collar. In contrast, under conditions of lower wettability—such as those observed with pure argon and helium—the molten metal spreads less, forming a taller and more concentrated collar around the stud.

The results shown in Table 3 confirm that CO_2 promotes a weld collar area nearly twice as large as that of pure argon, a result attributed to its enhanced wettability in the molten state. Furthermore, the addition of CO_2 to argon led to an increase of approximately 20 mm² in the collar area, reflecting a greater degree of material fusion. A comparison between CO_2 and helium shows that, despite their similar energy input and equivalent fusion levels, helium exhibits lower wettability due to its higher surface tension, which limits the lateral expansion of the molten material at the weld interface.

Table 3. *Wettability of the collar for different gases*

Gas	Sample 1 (mm²)	Sample 2 (mm²)	Sample 3 (mm²)	Average (mm²)
CO_2	181.70	154.41	131.85	155.99
He	112.951	90.348	96.421	99.907
C15	88.531	88.492	90.959	89.327
Ar	64.012	96.148	61.282	73.814

To analyze the weld collar formed under each shielding gas, macrographs were employed, enabling clear identification of differences in collar convexity resulting from the various gases used. In Figures 10a and 10b, a collar with high convexity is observed—characteristic of shielding gases with high surface tension, which limit the flow of molten metal and cause the material to concentrate around the stud.

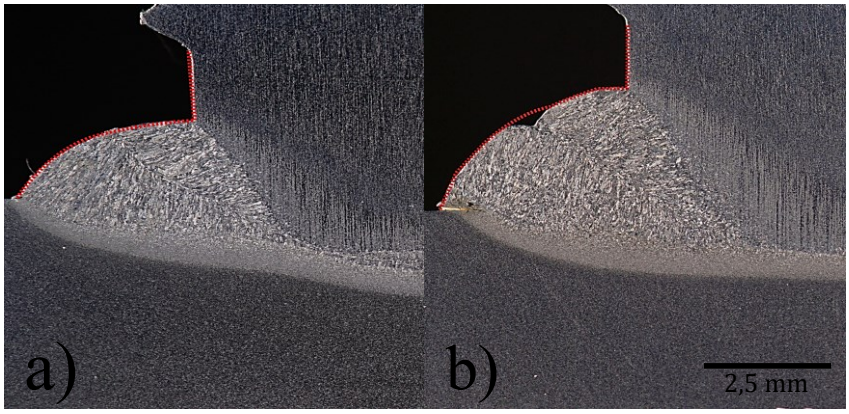

***Figure 10** - Welding Collar Formation a) Collar formed with pure helium, b) Collar formed with pure argon*

In contrast, the collars formed with the gases C15 (Figure 12a) and 100% CO_2, (Figure 12b), exhibit flatter profiles. In the case of pure CO_2, the effect of the pin dipping is evident, which results in the spreading of a large volume of molten material. This behavior is attributed to the reduction in surface tension provided by the gas, significantly increasing the fluidity of the molten metal. The addition of C15 (Figure 12a) highlights the impact of the 15% CO_2 in the mixture, which helps reduce the convexity of the collar.

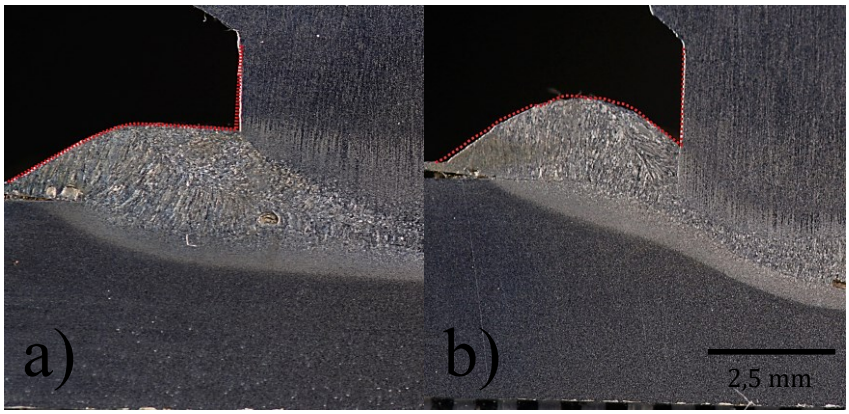

***Figure 11**- Welding Collar Formation a) Collar formed with C15 gas, b) Collar formed with pure CO_2*

4. CONCLUSION

Based on the results obtained, it was possible to evaluate the behavior of different shielding gases and their influence on energy efficiency, process stability, and weld quality.

Pure CO_2 and pure helium exhibited higher energy consumption, attributed to their physical and chemical properties, which led to elevated backside temperatures. In contrast, argon demonstrated lower energy consumption and reduced backside temperatures, indicating greater energy efficiency. The C15 mixture (85% argon and 15% CO_2) showed intermediate performance, with energy consumption and thermal behavior similar to that of argon.

Regarding process stability, the high-speed recordings revealed distinct characteristics for each gas. Pure CO_2 induced intense metallic vaporization, while pure helium ensured arc stability and molten tip control. Pure argon was notable for promoting cathodic cleaning and displaying high surface tension, which influenced droplet behavior. The C15

mixture demonstrated combined effects, enhancing wettability of the molten material but also showing occasional short circuits.

Finally, in terms of weld quality, pure CO_2 resulted in the highest penetration, with wider collars and increased stud fusion. Helium produced high penetration and more convex collars, with uniform fusion characteristics. Argon generated highly convex collars around the stud, but with lower penetration and fusion depth. The C15 mixture provided a balanced outcome, offering moderate penetration, controlled fusion, and an expanded collar area due to its improved wettability.

5. REFERENCES

ASM HANDBOOK COMMITTEE. Welding, brazing, and soldering. Vol. 6. ASM Handbook, 1993.

AMERICAN WELDING SOCIETY. Welding handbook: vol. 2: welding processes: gas, arc, and resistance. 5. ed. Editado por Arthur L. Phillips. Miami: American Welding Society, 1964.

CLARK, Jim. “Ionization Energies.” Chemistry LibreTexts, 29 jan. 2023. Disponível em: https://chem.libretexts.org/Bookshelves/Physical_and_Theoretical_Chemistry_Textbook_Maps/Supplemental_Modules_(Physical_and_Theoretical_Chemistry)/Physical_Properties_of_Matter/Atomic_and_Molecular_Properties/Ionization_Energy/Ionization_Energies. Acesso em: 27 nov. 2024.

INTERNATIONAL ORGANIZATION FOR STANDARDIZATION. ISO 14555:2017 - Welding — Arc stud welding of metallic materials. Genebra: ISO, 2017.

MARCHIONE, Tiago de Siqueira Lima. Desenvolvimento de ferramenta de suporte à parametrização do processo Stud Welding em aplicações com restrição térmica na indústria naval. 2024. 126 p. Dissertação (Mestrado em Engenharia Mecânica) — Programa de Pós-Graduação em Engenharia Mecânica, Universidade Federal de Santa Catarina, Florianópolis, 2024.

MODENESI, Paulo J. Introdução à Física do Arco Elétrico e sua Aplicação na Soldagem dos Metais. 2012.

MURPHY, Anthony B.; LOWKE, John J. Heat Transfer in Arc Welding.

ROTH, J. Reece. Industrial Plasma Engineering: Volume 1 - Principles. 1. ed. Boca Raton: CRC Press, 1995.

SCOTTI, Américo. Soldagem MIG/MAG: Melhor entendimento, melhor desempenho. 1. ed. São Paulo: Artliber, 2008. 284 p.

SCOTTI, A.; NASCIMENTO, A. S.; BATISTA, M. A.; NASCIMENTO, V. C. Comparação métodos para cálculo da potência elétrica através de uma abordagem experimental/matemática, em processos de soldagem a arco. In:

CONGRESSO IBEROAMERICANO DE ENGENHARIA MECÂNICA, 8., 2007, Cusco. Anais [...]. Cusco: [s.n.], 2007.

SCOTTI, A.; NASCIMENTO, A. S.; BATISTA, M. A.; NASCIMENTO, V. C. Comparação métodos para cálculo da potência elétrica através de uma abordagem experimental/matemática, em processos de soldagem a arco. In: CONGRESSO IBEROAMACTERICANO DE ENGENHARIA MECÂNICA, 8., 2007, Cusco. Anais [...]. Cusco: [s.n.], 2007.

Silva, Ezio & Scotti, Americo & Macedo Jr, José Rubens & Oliveira, Jose. (2011). Influência do Processo MIG/MAG na Qualidade da Energia Elétrica Fornecida pelas Concessionárias (Influence of GMAW Process in the Power Quality Supplied by the Utilities).

TRILLMICH, R.; WELZ, W. Stud welding: principles and application. Düsseldorf: DVS media GmbH, 2016.

ZEEMANN, A. Energia de Soldagem. Rio de Janeiro, 2003

ZIELINSKA, S.; PELLERIN, S.; VALENSI, F.; DZIERZEGA, K.; MUSIOL, K.; DE IZARRA, Ch.; BRIAND, F. Gas influence on the arc shape in MIG-MAG welding. European Physical Journal Applied Physics, v. 43, n. 1, p. 111-122, 2008. Disponível em: https://doi.org/10.1051/epjap:2008106. Acesso em: 2 dez. 2024.

6. RESPONSIBILITY FOR THE INFORMATION.

The author(s) is (are) solely responsible for the information included in this work.